Phosphorylation of the Light-Harvesting Complex II Isoform Lhcb2 Is Central to State Transitions

Longoni, Paolo; Douchi, Damien; Cariti, Federica; Fucile, Geoffrey; Goldschmidt-Clermont, Michel P.

How to cite

LONGONI, Paolo et al. Phosphorylation of the Light-Harvesting Complex II Isoform Lhcb2 Is Central to State Transitions. In: Plant physiology, 2015, vol. 169, n° 4, p. 2874–2883. doi: 10.1104/pp.15.01498

This publication URL: https://archive-ouverte.unige.ch/unige:86425

Publication DOI: 10.1104/pp.15.01498

Phosphorylation of the Lhcb2 isoform of Light Harvesting Complex II is central to state transitions

Paolo Longoni[1], Damien Douchi[1], Federica Cariti[1], Geoffrey Fucile[1] and Michel Goldschmidt-Clermont[1,2]

[1]Department of Botany and Plant Biology
University of Geneva
30 quai Ernest Ansermet, 1211 Genève 4, Switzerland

[2]iGE3, Institute of Genetics and Genomics of Geneva
University of Geneva, Switzerland

Running title: Contrasting phosphorylation of Lhcb1 and Lhcb2

One sentence summary:

Differential phosphorylation of the Lhcb1 and Lhcb2 subunits of the light harvesting antenna plays contrasting roles in photosynthetic light acclimation and supercomplex assembly.

Funding information

This work was supported by the University of Geneva, the Swiss National Fund for Scientific Research (grant 31003A_146300 / 1) and the Marie Curie ITN AccliPhot (GA 316427) of the European Union 7th Framework Program.

Corresponding author email:

michel.goldschmidt-clermont@unige.ch

List of author contributions:

P.L, D.D., F.C., G.F. and M.G.-C. designed the experiments; P.L, D.D., F.C., G.F. performed the experiments; P.L. , G.F. and M.G.-C. wrote the article.

Abstract

Light harvesting complex II (LHCII) is a crucial component of the photosynthetic machinery, with central roles in light capture and acclimation to changing light. The association of a LHCII trimer with Photosystem I in the PSI-LHCII supercomplex is strictly dependent on LHCII phosphorylation mediated by the kinase STN7, and is directly related to the light acclimation process called state transitions. In *Arabidopsis thaliana* the LHCII trimers contain isoforms that belong to three classes: Lhcb1, Lhcb2, and Lhcb3. Only Lhcb1 and Lhcb2 can be phosphorylated in the N-terminal region. Here we present an improved Phos-tag™-based method to determine the absolute extent of phosphorylation of Lhcb1 and Lhcb2. Both classes show very similar phosphorylation kinetics during state transition. Nevertheless, only Lhcb2 is extensively phosphorylated (>98%) in PSI-LHCII, whereas phosphorylated Lhcb1 is largely excluded from this supercomplex. Both isoforms are phosphorylated to different extents in other photosystem supercomplexes and in different domains of the thylakoid membranes. The data imply that despite their high sequence similarity, differential phosphorylation of Lhcb1 and Lhcb2 plays contrasting roles in light acclimation of photosynthesis.

Introduction

Light capture and its conversion to chemical energy occur in a set of transmembrane protein complexes of the thylakoid membrane. Photosystem II (PSII), the cytochrome b_6f complex and Photosystem I (PSI) drive photosynthetic electron flow and the creation of a proton gradient across the thylakoid membrane. ATP synthase couples the dissipation of this gradient to the synthesis of ATP. The light harvesting antennae play an important role in collecting light and transferring energy to the photosystems. Light Harvesting Complex I (LHCI) exclusively transfers light energy to PSI, with which it is tightly associated (Croce and van Amerongen, 2014). In contrast Light Harvesting Complex II (LHCII), which is the most abundant complex of the thylakoid membrane, can transfer energy to PSI or PSII (Grieco et al., 2015). Light is highly variable in natural environments and plants experience continuous changes in both its spectrum and intensity on timescales as short as seconds. Changes in light quality may unbalance the activity of the two photosystems since their absorption spectra differ, while high light intensity can lead to over-excitation and induce photodamage. At low or moderate light intensities, the LHCII complex differentially associates with PSII or PSI, in a phosphorylation-dependent process known as state transitions, to rapidly respond to changes in the spectrum of light. Briefly, under light quality that activates PSII more than PSI (*e.g.* blue light), LHCII is phosphorylated and as a consequence its binding to PSI is favoured (state 2). Conversely, under light that preferentially excites PSI (enriched in far-red) this association can be reverted by de-phosphorylation of the LHCII antenna which favours its binding to PSII (state 1) (Goldschmidt-Clermont and Bassi, 2015; Kim et al., 2015). A protein kinase, STN7, and a protein phosphatase, PPH1/TAP38, are essential for the rapid

phosphorylation and dephosphorylation of the LHCII antenna that regulate its differential association to PSI or PSII (Bellafiore et al., 2005; Pribil et al., 2010; Shapiguzov et al., 2010). Only a relatively small fraction of the LHCII antenna (< 20%) is estimated to participate in state transitions in *A. thaliana* (Allen, 1992). However the process is conserved across the green eukaryotes and is relevant to plant fitness (Frenkel et al., 2007). Under high light, energy-dependent quenching of LHCII predominates and furthermore this antenna can uncouple from PSII (Wientjes et al., 2013a).

The differential association of photosystems, LHCII and other components of the thylakoid membrane gives rise to a set of supercomplexes that are central in assuring photosynthetic efficiency and a rapid response to environmental cues (Caffarri et al., 2009; Duffy et al., 2013; Pietrzykowska et al., 2014; Fristedt et al., 2015). Fine-tuning the dynamic assembly of these supercomplexes involves the association of antennae containing specific sets of Lhcb proteins. The major LHCII antenna comprises homo- and hetero-trimers of Lhcb1, Lhcb2 and Lhcb3 (Jackowski et al., 2001), while the minor LHCII isoforms (Lhcb4, Lhcb5 and Lhcb6) are monomeric (de Bianchi et al., 2008). Lhcb1, Lhcb2 share very similar primary structure and associated pigments (Formaggio et al., 2001; Zhang et al., 2008) while Lhcb3 appears to have slightly different features (Standfuss and Kühlbrandt, 2004). In *Arabidopsis thaliana*, 5 genes encode Lhcb1 isoforms, 3 genes encode Lhcb2 isoforms, and a single gene encodes Lhcb3. The principal discriminant between these classes is a short stretch of residues at the N-terminal end, which is of particular importance since it contains the threonine that is reversibly phosphorylated during light acclimation processes (Goldschmidt-Clermont and Bassi, 2015). During evoulution, land plants have maintained a major LHCII composed of different class of Lhcb subunits. The phosphorylated N-terminus of Lhcb2 was particularly well conserved (Alboresi et al., 2008; Zhang et al., 2008).

PSII-LHCII supercomplexes have been isolated from Arabidopsis with up to 4 LHCII trimers bound to a PSII dimer, as well as the three minor monomeric antennae (Lhcb4, Lhcb5 and Lhcb6) (Caffarri et al., 2009; Kouřil et al., 2012). In the LHCII trimers of these supercomplexes different classes of Lhcb subunits are differently distributed suggesting a specific role in light acclimation for each of them (Damkjær et al., 2009; Pietrzykowska et al., 2014). In the stably bound S trimer Lhcb1 and Lhcb2 are more abundant, while the moderately bound M trimer contains mostly Lhcb1 and Lhcb3 (Galka et al., 2012). PSII supercomplexes isolated from spinach showed the presence of an extra LHCII trimer (L trimer), therefore it is possible that in Arabidopsis also other trimers are associated to the PSII dimer in a more labile supercomplex that cannot be isolated (Boekema et al., 1999). A single LHCII trimer, containing Lhcb1 and Lhcb2, stably associates with PSI to constitute the PSI-LHCII supercomplex, whose formation is dependent on LHCII phosphorylation by STN7 in state 2 (Kouřil et al., 2005a; Galka et al., 2012).

Previous reports have shown that the relative phosphorylation of Lhcb1 and Lhcb2 isoforms differs amongst thylakoid supercomplexes (Galka et al., 2012; Leoni et al., 2013). Here we address the specific

roles of Lhcb1 and Lhcb2 phosphorylation in photosynthetic acclimation. The improved protocol for SDS-PAGE in the presence of Phos-tag™ that we present allows quantification of the extent of phosphorylation for each class of antenna isoforms. We report that in the PSI-LHCII supercomplex that is assembled in state 2, only the phosphorylated form of Lhcb2 is present, while the phosphorylated form of Lhcb1 is excluded. In contrast both Lhcb1 and Lhcb2 are phosphorylated to different levels in other supercomplexes. This quantitative information on the level of phosphorylation of Lhcb1 and Lhcb2 offers new insights into the specific roles of the two classes of LHCII isoforms in light acclimation and supercomplex formation.

Results

An improved Phos-tag™ PAGE protocol allows a quantitative measurement of antenna phosphorylation

Phos-tag™ together with a chelated divalent cation such as Zn^{2+} binds phosphate groups. Thus using electrophoresis in poly-acrylamide gels containing immobilized Phos-tag™ (Phos-tag™ PAGE), phosphorylated proteins can be resolved from their non-phosphorylated form because their migration is selectively retarded (Bekesova et al., 2015). Although the different phosphorylated forms are separated, it remains difficult to quantify by immunoblotting their abundance relative to the non-phosphorylated protein. The main reason is that since Phos-tag™ retards the phosphoprotein during electrophoresis, it also hampers its subsequent transfer to a membrane, leading to incomplete transfer of the phosphorylated form and therefore to an underestimation of phosphorylation. This problem can be partly alleviated by incubating the gel in EDTA-containing solution to strip Zn^{2+} prior to the transfer (Kinoshita et al., 2009). Here we use an improved protocol, with a two-layer resolving gel containing the Phos-tag™ ligand only in the upper portion. Phosphoproteins are retarded during their migration through the upper layer and then enter the lower layer, from which they can be transferred to a membrane without the interference of Phos-tag™.

Using the two-layer Phos-tag™ PAGE protocol, phosphorylated Lhcb1 (P-Lhcb1) and Lhcb2 (P-Lhcb2) were resolved from the unphosphorylated forms (Fig. 1). The regulation of LHCII trimer binding to different photosystem supercomplexes involves phosphorylation of a single threonine residue at position 3, from the N-terminus generated after removal of the transit peptide (Rochaix, 2014). Immuno-blotting with phospho-specific antibodies against P-Lhcb1 or P-Lhcb2 confirmed that the upper band represents the protein with the N-proximal threonine phosphorylation (Fig. 1) (Leoni et al., 2013). The major LHCII isoforms constitute a peculiar substrate for immuno-detection: the only portion suitable to raise antibodies for a specific Lhcb class is the N-terminus of the mature polypeptide, since the remaining portion shares very high sequence similarity with other Lhcb isoforms as well as with other antenna proteins. Thus the Lhcb1 antibodies probably fail to recognize Lhcb1.4, due to its N-terminal sequence which differs from the other Lhcb1 variants. Moreover the N-terminal peptide used as antigen to raise isoform-specific antisera against Lhcb1

and Lhcb2 contains the phosphorylation site at threonine 3. It appeared likely that the presence or absence of phosphorylation might influence recognition by the antisera. In order to assess this possible bias, the proteins transferred on the immunoblot membrane were subsequently treated with λ protein phosphatase. Indeed with the antiserum against Lhcb2, phosphatase treatment of the membrane enhanced the signal of the phosphorylated form of the protein more than two-fold (Supplemental Fig. 1). This treatment did not influence the signal for Lhcb1. After incubation with λ phosphatase, the signal obtained with phosphospecific antibodies against P-Lhcb1 or P-Lhcb2 became undetectable, showing that dephosphorylation of these proteins on the membrane was essentially complete (Supplemental Fig. 1). The phosphatase treatment of the membrane blot was therefore included in our improved protocol that was used in all further experiments.

To determine the phosphorylation levels of Lhcb1 and Lhcb2, it is important to determine whether the respective antibodies are specific. This was previously shown in an analysis of antisense lines deficient inLhcb1 or Lhcb2 (Pietrzykowska et al. 2014). The lack of cross-reactivity was further confirmed using recombinant proteins expressed in *Escherichia coli* (Supplemental Fig. 2). To obtain quantitative data from immunoblotting, it is necessary to determine whether the signal is proportional to the amount of protein and in what range. Using different amounts of protein extracts with different levels of protein phosphorylation, there was a linear correlation between the signal obtained with the Lhcb1 or Lhcb2 antisera and the amount of total protein up to at least 5 µg with our protocol (Supplemental Fig. 3).

The two-layer Phos-tag™ PAGE protocol offers better transfer of the proteins from the Phos-tag™ -free part of the resolving gel to the membrane and therefore a reliable quantification of phosphorylation. This was confirmed for Lhcb1 and Lhcb2 as follows (Supplemental Fig. 4). Samples with widely different extents of phosphorylation were subjected to two-layer Phos-tag ™ PAGE and immunoblotting. For each sample, the sum of the signals of the phosphorylated and non-phosphorylated forms was normalized to the signal of actin, the loading control. This normalized sum remained nearly constant over the whole range of phosphorylation levels, indicating that there was no significant bias in the transfer of the phosphorylated form. If the phosphorylated form had been inefficiently transferred, a decrease of this sum with increasing phosphorylation would have been expected.

In summary, three control experiments validate the improved protocol for quantification of the extent of phosphorylation of Lhcb1 or Lhcb2: (i) the retarded band corresponds to the phosphorylated form, (ii) there is a linear correlation of the signal with the amount of protein loaded, and (iii) the sum of the signals of the phosphorylated and non-phosphorylated forms is nearly constant over a wide range of phosphorylation levels.

Lhcb1 and Lhcb2 have different phosphorylation levels

Although it is known that both Lhcb1 and Lhcb2 are phosphorylated, principally by the STN7 kinase, the extent of this phosphorylation for each class of LHCII antenna subunits was not known (Leoni et al., 2013). In 6 week-old plants exposed to low intensity white light (70 µmol s^{-1} m^{-2}) the phosphorylation level of the two LHCII subunits was remarkably different (Fig. 2). Only a small fraction of Lhcb1 was phosphorylated (13 ±3 %), while Lhcb2 was more extensively phosphorylated (45 ±6 %) (n=5). In order to verify the effect of the lack of STN7, the major kinase acting on the antenna proteins, and of PPH1/TAP38, the main counteracting phosphatase, mutants for either protein were compared in terms of total phosphorylation level (Bellafiore et al., 2005; Shapiguzov et al., 2010). While in the *stn7* kinase mutant phosphorylation of Lhcb1 and Lhcb2 was reduced below detection level, in the *pph1*/*tap38* phosphatase mutant the fraction of phosphorylated Lhcb1 showed no difference compared to the wild-type value and a slight increase in the Lhcb2 phosphorylation level was not statistically significant (P>0.10) (Fig. 2).

To increase antenna phosphorylation, mature leaves of adult plants were first subjected to 60 minutes of far-red light to favor PSI (state 1), followed by 60 minutes of blue light to preferentially excite PSII (state 2). The phosphorylated fraction of Lhcb1 increased to 31 ±4 % while the phosphorylated portion of Lhcb2 was 54 ± 4% (n=4) (Supplemental Fig. 5). The same light regime applied to 15 day-old seedlings revealed a very similar phosphorylation trend (Fig. 3). The final phosphorylation level was not different from that observed in adult leaves for Lhcb1 (34 ±8 %), while for Lhcb2 it was even higher (69 ±12 %; P<0.05; n=5). It was previously reported that in different plant species, including Arabidopsis, the kinetics of phosphorylation in a transition from state 1 to state 2 were faster for Lhcb2 compared to Lhcb1 (Jansson et al., 1990; Leoni et al., 2013). Here the phosphorylation kinetics of the two subunits were measured during the shift from far-red to blue light in Arabidopsis 15 day-old seedlings (Fig. 3). The two antenna isoforms did not show a large difference in their relative phosphorylation kinetics, but differed in the final level of phosphorylation, with Lhcb2 more extensively phosphorylated than Lhcb1 (Fig. 3). Similar phosphorylation dynamics were observed in 6 week-old plants, even though the final level of phosphorylation was lower, as described above (Supplemental Fig. 5).

Phosphorylation of antenna isoforms in different supercomplexes

The phosphorylation of Lhcb1 and Lhcb2 in PSI and PSII supercomplexes was investigated using two-dimensional gel electrophoresis. Blue native polyacrylamide gel electrophoresis (BN-PAGE) allows the separation of the main supercomplexes containing PSI or PSII associated with LHCII trimers. Using different detergents, specifically digitonin or β-dodecylmaltoside (β-DM), it is possible to solubilize different fractions of the thylakoid membranes and thus to resolve a different set of supercomplexes (Järvi et al., 2011; Grieco et al., 2015). Digitonin releases the complexes from stromal lamellae and grana margins where most of PSI localizes, whereas β-DM also solubilizes the complexes in grana cores containing mostly PSII. The lanes

obtained after BN-PAGE were used in a second dimension using two-layer Phos-tag ™ PAGE (2D electrophoresis) in order to determine the degree of phosphorylation of the antenna isoforms in the different supercomplexes. More extensive phosphorylation of both Lhcb1 and Lhcb2 was observed in the supercomplexes solubilized after digitonin treatment compared to those obtained after β-DM treatment (Fig. 4). In the digitonin extract Lhcb2 appeared more phosphorylated than Lhcb1 in all the supercomplexes (higher P to U ratio in the 2D gel). Remarkably, Lhcb2 was phosphorylated to a very high extent when associated with the PSI-LHCII supercomplex, which is assembled upon antenna phosphorylation by STN7 in state 2. On the contrary after β-DM solubilization the supercomplexes from the grana cores, mostly containing PSII-LHCII, showed little LHCII phosphorylation while most of the phosphorylated antenna was present in the free trimers (Fig. 4). To determine whether increased phosphorylation of the LHCII trimers would change the pattern of phosphorylation in the supercomplexes that can be recovered, thylakoids were prepared from *pph1-3* plants lacking the LHCII phosphatase, after a light shift from far-red to blue. For the supercomplexes extracted with digitonin, the phosphorylation pattern obtained after two-dimensional gel electrophoresis did not noticeably change (Fig. 4). However, a difference was apparent for the grana-core supercomplexes extracted with β-DM. In the *pph1-3* mutant, Lhcb2 phosphorylation increased in the PSII-LHCII supercomplexes with a clear trend: smaller complexes contained more extensively phosphorylated Lhcb2 than larger ones.

The different abundance of Lhcb1 and Lhcb2 in the digitonin-extracted supercomplexes hinders the estimation of their respective phosphorylation levels by 2D electrophoresis. Furthermore the shape of the spots leads to saturation of strong signals and a reduced range of linearity for the immunoblot assay. In order to confirm the observations and obtain quantitative estimates of the phosphorylation status of Lhcb1 and Lhcb2 in different supercomplexes, each band was cut after BN-PAGE of a digitonin extract, ground in SDS buffer and the supernatant was then subjected to two-layer Phos-tag™ PAGE (Fig. 5). As suggested by the results of two-dimensional gel electrophoresis, the PSI-LHCII supercomplex showed a unique phosphorylation pattern for the two classes of major LHCII isoforms. Lhcb2 was almost completely phosphorylated (over 98% in phosphorylated form) while Lhcb1 was essentially unphosphorylated (<1%) (Supplemental Fig. 6). This is in agreement with the results in Figure 4, where in the PSI-LHCII complex Lhcb2 was also strongly phosphorylated, while phosphorylated Lhcb1 was barely detectable compared to the strong and apparently saturated signal of its unphosphorylated form. It should be noted here that the completely different patterns of phosphorylation confirm that the two antibodies are specific for their respective targets and do not show significant cross-reactivity. Bands containing the PSII-LHCII supercomplexes extracted with β-DM from grana cores were also analysed individually for antenna phosphorylation (Supplemental Fig. 7). This confirmed the observations from the 2D-gels showing that Lhcb2 is more phosphorylated in the smaller PSII-LHCII supercomplex containing only one LHCII trimer than in the larger supercomplex containing two trimers.

It is important to note that this specific differential phosphorylation was unique to the PSI-LHCII supercomplex, since both Lhcb1 and Lhcb2 were present in partially phosphorylated form in other supercomplex-containing bands, with Lhcb2 generally more phosphorylated than Lhcb1 (Fig. 5). A relatively high level of Lhcb1 and Lhcb2 phosphorylation was observed in the supercomplex Sc4b band and in the megacomplex Mc5b band. Both were described to contain PSI, PSII and LHCII, but fluorescence lifetime analysis indicated that PSII may not be functionally connected to PSI in these bands (Järvi et al., 2011; Yokono et al., 2015).

Discussion

Phosphorylation kinetics of Lhcb1 and Lhcb2

State transitions provide a rapid acclimatory response to changes in light quality and operate in the time range of a few minutes. Because of the different roles of Lhcb1 and Lhcb2 in the state transition supercomplex, it was of interest to examine the kinetics of their phosphorylation, which is in both cases dependent on the protein kinase STN7. It was previously reported that Lhcb2 is phosphorylated at a faster rate than Lhcb1 in Arabidopsis (Larsson et al., 1987; Leoni et al., 2013). However, when relative rates were compared in our work using two-layer Phos-tag™ PAGE, Lhcb1 and Lhcb2 were phosphorylated with very similar kinetics (Fig. 3). A possible reason for the discrepancy might be the light conditions used. In our study state 1 was induced with far-red light only and state 2 by shifting to blue light, while in the previous work far-red was added to a red light background. It is possible that our conditions led to a more complete antenna dephosphorylation in state 1. The availability of the Lhcbs as substrates for the kinase may change under different light conditions (Zer et al., 2003; Kirchhoff, 2014). Furthermore, it should be pointed out that Lhcb2 is less abundant than Lhcb1. Thus its higher phosphorylation level compared to Lhcb1 and its similar phosphorylation kinetics suggest that Lhcb2 is preferentially phosphorylated and appears to be a better substrate for the kinase(s) in terms of accessibility or recognition.

Antenna phosphorylation in the PSI-LHCII state transition supercomplex.

Some caution should be used in interpreting the phosphorylation of photosynthetic supercomplexes solubilized by detergent treatment of thylakoid membranes and isolated by BN-PAGE. Several interrelated effects should be considered which include the role of phosphorylation in the regulated assembly of the complexes and on their stability *in vivo*, but also the effect of phosphorylation on the lability of the complexes *in vitro* upon detergent extraction. Indeed after BN-PAGE, a large proportion of LHCII is in the form of free trimers, which are most likely loosely bound in supercomplexes *in vivo* (Caffarri et al., 2009; Järvi et al., 2011; Pagliano et al., 2014; Grieco et al., 2015). Furthermore PSII supercomplexes in the grana core may not be accessible to phosphorylation for steric reasons, because the tight appression of the membranes could hinder the access of the corresponding protein kinases (Zer et al., 2003; Kirchhoff, 2014).

The PSI-LHCII complex assembles in state 2 and involves the binding of a mobile trimer, which contains Lhcb1 and Lhcb2 (Galka et al., 2012), to the PSI complex. This association depends on the kinase STN7. An analysis of Arabidopsis knock-down lines lacking Lhcb1 or Lhcb2 previously suggested that the two isoforms play complementary roles in state transitions. Lhcb1 could largely replace Lhcb2 in the lines lacking Lhcb2, but they could not assemble the PSI-LHCII supercomplex or undergo state transitions (Pietrzykowska et al., 2014). It was also observed using phospho-specific antisera that PSI-LHCII is enriched in P-Lhcb2 but lacks P-Lhcb1 (Leoni et al., 2013). While such antibodies could reveal relative differences in phosphorylation under different conditions or in different complexes, our two-layer Phos-tag™ PAGE method now allows a quantitative assessment of the absolute extent of phosphorylation.

We observed that in the PSI-LHCII supercomplex Lhcb2 is in fact almost entirely phosphorylated (>98 %), while in contrast Lhcb1 is not phosphorylated to measurable levels (<1%) (Fig. 5 and Supplemental Fig. 6). This implies that phosphorylation of Lhcb2 is key to the formation of PSI-LHCII. For state transitions, the reversible allocation of LHCII to the photosystems has been interpreted as a change in the relative affinity of the mobile LHCII trimer for PSI versus PSII (Haldrup et al., 2001). In this perspective, the formation or stability of the PSI-LHCII thus appears to depend on the phosphorylation of Lhcb2 and the lack of phosphorylation of Lhcb1. It cannot however be excluded that PSI-LHCII complexes with both isoforms phosphorylated could assemble *in vivo*, but would be lost upon detergent solubilisation and BN-PAGE because of a low stability.

It is also striking that the phosphorylated form of Lhcb1 is largely excluded from the PSI-LHCII supercomplex (Fig. 4), even though the presence of Lhcb1 appears to be crucial, since in knock-down lines lacking this isoform the supercomplex does not form (Pietrzykowska et al., 2014). The lack of Lhcb1 phosphorylation in PSI-LHCII could seem somewhat paradoxical, since STN7-dependent phosphorylation of both Lhcb1 and Lhcb2 is observed in conditions that favor a transition from state 1 to state 2 (Fig. 2) (Leoni et al., 2013). An extreme view might be that phosphorylation of Lhcb2 is central, and that phosphorylation of Lhcb1 is a collateral effect, with no specific function, due to the imperfect substrate specificity of the kinase(s) and phosphatase(s). However it is also possible and perhaps more likely that phosphorylation of Lhcb1 is important in the regulation of other supercomplexes, and/or of their localization in different domains of the thylakoid network.

Antenna phosphorylation in the PSII-LHCII supercomplexes

In the PSII-LHCII supercomplexes solubilized with β-DM from grana membranes, the phosphorylation of Lhcb1 and Lhcb2 is low. However after a far-red to blue shift that induces high levels of phosphorylation, there is a clear difference in Lhcb2 phosphorylation between complexes of different sizes (Fig. 4 and

Supplemental Fig. 7). Phosphorylation of Lhcb2 is higher in complexes containing only one LHCII trimer, and gradually lower in complexes containing two or three trimers (Fig. 6). This could suggest that PSII-LHCII supercomplexes with high levels of LHCII trimer phosphorylation are less stable *in vivo*, or labile during extraction. An alternate possibility is that in the smaller PSII-LHCII complexes, Lhcb2 is more accessible to the kinase, while in contrast it is more deeply buried in the larger complexes. The latter hypothesis would fit with the previous observation that Lhcb2 is more abundant in the trimer (named S) most closely associated to the PSII core (Galka et al., 2012). However, Lhcb1 is more phosphorylated in large PSII-rich supercomplexes solubilized with digitonin from stromal lamellae and grana margins, while its level of phosphorylation in PSII-LHCII supercomplexes extracted with β-DM from grana cores is comparatively low (Fig. 6) (Yokono et al., 2015). These observations suggest that Lhcb phosphorylation may contribute to the movement of the PSII-LHCII supercomplexes from grana cores towards less stacked domains of the thylakoid membrane, grana margins and stromal lamellae. This hypothesis is consistent with the recent proposal that phosphorylation of both the LHCII antenna and the PSII core assist the migration of PSII-LHCII out of grana (Mekala et al., 2015). The phosphorylation patterns of Lhcb1 and Lhcb2 may be rationalized by considering that in low levels of white light, energy capture should be maximized by ensuring that all LHCII trimers are associated with photosystems. This would require a higher degree of Lhcb2 phosphorylation in the stromal lamellae and grana margins to promote binding of LHCII to PSI, and a lower level of Lhcb1 and Lhcb2 phosphorylation in the grana cores to avoid interference with the supramolecular organization of PSII-LHCII supercomplexes (Wientjes et al., 2013b). Under blue light and the ensuing transition towards state 2, a higher degree of Lhcb2 phosphorylation would increase the formation of the PSI-LHCII state-transition complex in the grana margins, and possibly favour the dissociation of the higher-order PSII-LHCII supercomplexes in the grana cores (Dietzel et al., 2011).

In conclusion the optimized Phos-tag™ system presented in this work allows a detailed analysis of the phosphorylation of proteins of interest, and allows a better understanding of the role and kinetics of protein phosphorylation. Finally it should be emphasized that the contrasting phosphorylation of Lhcb1 and Lhcb2 in different photosynthetic supercomplexes implies that in examining the physiology of light acclimation, it may be misleading to consider LHCII phosphorylation in bulk and it is rather the phosphorylation of specific isoforms that should be taken into account.

Methods

Plant material and light conditions

Arabidopsis thaliana ecotype Columbia (hereafter Arabidopsis) plants were grown for 40 days at 22°C and 65% RH under white light (70 µmol sec^{-1} m^{-2}) with 8h daylight. The light treatments were initiated 4h after

the beginning of the light period. 15-day old plantlets were grown at 22°C under white light (70 µmol sec^{-1} m^{-2}) with 16h daylight in a growth chamber (Percival CU36L5) on Murashige-Skoog agar plates supplemented with 1% sucrose. The mutant lines of PPH1/TAP38 and STN7 were previously described as *pph1-3* (Shapiguzov et al., 2010) and *stn7* (Bellafiore et al., 2005). For far-red and blue light treatment the plants were placed under LED panels (L735 andL470, Epitex).

Two-layer Phos-tag™ PAGE

Total protein extract from seedlings or leaves was prepared as previously described (Samol et al., 2012). The total protein concentration was measured with bicinchoninic acid solution (Sigma-Aldrich) following the manufacturer's instructions. All the chemicals were bought from Applichem-Panreac unless otherwise stated. The gel was prepared as follows. Heavy resolving-gel solution: 357 mM Bis-Tris (pH 6.8) (Roth), 30% w/v glycerol, 9% Acrylamide/bis-Acrylamide 37.5:1, 0.05% v/v TEMED, 0.025% w/v ammonium persulfate (APS). Light resolving-gel solution: 357 mM Bis-Tris (pH 6.8), 8% Acrylamide/bis-Acrylamide 37.5:1, 60 µM Phos-Tag™ (Wako chemicals), 0.05% v/v TEMED, 0.05% w/v APS, 0.01% w/v coomassie brilliant blue G-250 (Bio-Rad). Stacking-gel solution: 357 mM Bis-Tris (pH 6.8), 4% Acrylamide/bis-Acrylamide 37.5:1, 0.1% v/v TEMED, 0.05% w/v APS.

Three volumes of the heavy solution were poured between the gel plates, followed by one volume the light solution. The two solutions were partially mixed with a nylon membrane in order to smooth the interface between the two layers. After the two-layer resolving gel polymerized the stacking gel was cast. Samples were prepared in LDS Loading buffer (10% glycerol w/v, 244 mM Tris HCl (pH 8.5), 2% LDS, 0.33 mM coomassie brilliant blue G-250, 100 mM di-thio threitol (DTT)) and heated for 5 minutes at 70°C before loading. 5 µg of total protein sample was loaded per well. The PAGE was performed with freshly prepared running buffer (61 mM Tris, 50 mM MOPS, 0.1% (w/v) SDS and 5 mM sodium bisulfite).

The gel was transferred overnight (16h) onto a nitrocellulose membrane in a tank containing transfer buffer (500mM Bicine (Sigma-Aldrich), 500mM Bis-tris, 20mM EDTA, 10% Methanol, 5mM sodium bisulfite, pH7.2). After staining with amido black (0,1% Amido Black 10B in 30% methanol (v/v), 10% acetic acid (v/v)), the membrane was treated with blocking buffer (3% bovine serum albumin, 1x TBS (50 mM Tris-Cl, pH 7.5; 150 mM NaCl), 0.1% Triton x100) for 40 minutes with agitation. For dephosphorylation the membrane was incubated in blocking buffer with 400 U/mL of λ protein phosphatase (New England BioLabs), 2mM DTT, 2mM $MnCl_2$ for 4h at room temperature. The membrane was washed twice with PBS and with deionized water before incubation with the primary antibody. For immunodetection the Lhcb1 (AS09 522), Lhcb2 (AS01 003), Lhcb1-P (AS13 2704) and Lhcb2-P (AS13 2705) antibodies were from Agrisera, and the actin antibody (A0480) from Sigma-Aldrich. After incubation with the secondary antibody (Promega) and ECL reagent, the chemiluminescence was detected using a LAS-4000 Mini cooled CCD camera. Band intensity was measured with ImageQuant and ImageJ softwares.

Isolation of thylakoid membranes

Thylakoid membranes from 40-day old Arabidopsis plants were isolated as previously described (Arnold et al., 2014). Detergent solubilization was performed with 1% Digitonin (Sigma-Aldrich) or 1% β-Dodecylmaltoside (Calbiochem) as previously described (Järvi et al., 2011). Native gels for supercomplex separation was prepared as described (Schägger and von Jagow, 1991) using an acrylamide:bis-acrylamide ratio of 37.5:1, an acrylamide gradient of 3.5–12.5% (w/v) in the resolving gel and an acrylamide concentration of 3% (w/v) in the stacking gel. The second dimension PAGE was performed as previously described (Järvi et al., 2011). Excised bands were ground with a pestle in Laemmli Buffer (138 mM Tris/HCl (pH 6.8), 6 M urea, 22.2% glycerol (w/v), 4.3% SDS (w/v) and 5% 2-mercaptoethanol(v/v)), incubated for 1h at 70°C and then centrifuged in a microfuge. The supernatant was diluted 1 to 1 with 2xLDS loading buffer (20% Glycerol, 500mM Tris-HCl (pH 8.5), 4% LDS (w/v), 0.66 mM Coomassie Blue G250, 200 mM DTT), and appropriate volumes (5 – 20 µl) were loaded for two-layer Phos-Tag™ PAGE as described above.

Acknowledgements

We thank Jean-David Rochaix for scientific advice and comments on the manuscript, and Lorenzo Ferroni for contributing to the optimization of Blue Native PAGE.

References

Alboresi A, Caffarri S, Nogue F, Bassi R, Morosinotto T (2008) In Silico and Biochemical Analysis of Physcomitrella patens Photosynthetic Antenna: Identification of Subunits which Evolved upon Land Adaptation. PLoS ONE 3: e2033

Allen JF (1992) Protein phosphorylation in regulation of photosynthesis. Biochim Biophys Acta 1098: 275–335

Arnold J, Shapiguzov A, Fucile G, Rochaix J-D, Goldschmidt-Clermont M, Eichacker LA (2014) Separation of Membrane Protein Complexes by Native LDS-PAGE. Plant Proteomics. Springer, pp 667–676

Bekesova S, Komis G, Krenek P, Vyplelova P, Ovecka M, Luptovciak I, Illes P, Kucharova A, Samaj J (2015) Monitoring protein phosphorylation by acrylamide pendant Phos-Tag™ in various plants. Tech Adv Plant Sci 6: 336

Bellafiore S, Barneche F, Peltier G, Rochaix J-D (2005) State transitions and light adaptation require chloroplast thylakoid protein kinase STN7. Nature 433: 892–895

de Bianchi S, Dall'Osto L, Tognon G, Morosinotto T, Bassi R (2008) Minor Antenna Proteins CP24 and CP26 Affect the Interactions between Photosystem II Subunits and the Electron Transport Rate in Grana Membranes of Arabidopsis. Plant Cell 20: 1012–1028

Boekema EJ, van Roon H, van Breemen JFL, Dekker JP (1999) Supramolecular organization of photosystem II and its light-harvesting antenna in partially solubilized photosystem II membranes. Eur J Biochem 266: 444–452

Caffarri S, Kouřil R, Kereïche S, Boekema EJ, Croce R (2009) Functional architecture of higher plant photosystem II supercomplexes. EMBO J 28: 3052–3063

Croce R, van Amerongen H (2014) Natural strategies for photosynthetic light harvesting. Nat Chem Biol 10: 492–501

Damkjær JT, Kereïche S, Johnson MP, Kovacs L, Kiss AZ, Boekema EJ, Ruban AV, Horton P, Jansson S (2009) The Photosystem II Light-Harvesting Protein Lhcb3 Affects the Macrostructure of Photosystem II and the Rate of State Transitions in Arabidopsis. Plant Cell 21: 3245–3256

Dietzel L, Bräutigam K, Steiner S, Schüffler K, Lepetit B, Grimm B, Schöttler MA, Pfannschmidt T (2011) Photosystem II Supercomplex Remodeling Serves as an Entry Mechanism for State Transitions in Arabidopsis. Plant Cell 23: 2964–2977

Duffy CDP, Valkunas L, Ruban AV (2013) Light-harvesting processes in the dynamic photosynthetic antenna. Phys Chem Chem Phys PCCP 15: 18752–18770

Formaggio E, Cinque G, Bassi R (2001) Functional architecture of the major light-harvesting complex from higher plants1. J Mol Biol 314: 1157–1166

Frenkel M, Bellafiore S, Rochaix J-D, Jansson S (2007) Hierarchy amongst photosynthetic acclimation responses for plant fitness. Physiol Plant 129: 455–459

Fristedt R, Herdean A, Blaby-Haas CE, Mamedov F, Merchant SS, Last RL, Lundin B (2015) PHOTOSYSTEM II PROTEIN33, a Protein Conserved in the Plastid Lineage, Is Associated with the Chloroplast Thylakoid

Membrane and Provides Stability to Photosystem II Supercomplexes in Arabidopsis. Plant Physiol 167: 481–492

Galka P, Santabarbara S, Khuong TTH, Degand H, Morsomme P, Jennings RC, Boekema EJ, Caffarri S (2012) Functional Analyses of the Plant Photosystem I–Light-Harvesting Complex II Supercomplex Reveal That Light-Harvesting Complex II Loosely Bound to Photosystem II Is a Very Efficient Antenna for Photosystem I in State II. Plant Cell Online 24: 2963–2978

Goldschmidt-Clermont M, Bassi R (2015) Sharing light between two photosystems: mechanism of state transitions. Curr Opin Plant Biol 25: 71–78

Grieco M, Suorsa M, Jajoo A, Tikkanen M, Aro E-M (2015) Light-harvesting II antenna trimers connect energetically the entire photosynthetic machinery — including both photosystems II and I. Biochim Biophys Acta BBA - Bioenerg 1847: 607–619

Haldrup A, Jensen PE, Lunde C, Scheller HV (2001) Balance of power: a view of the mechanism of photosynthetic state transitions. Trends Plant Sci 6: 301–305

Jackowski G, Kacprzak K, Jansson S (2001) Identification of Lhcb1/Lhcb2/Lhcb3 heterotrimers of the main light-harvesting chlorophyll a/b-protein complex of Photosystem II (LHC II). Biochim Biophys Acta 1504: 340–345

Jansson S, Selstam E, Gustafsson P (1990) The rapidly phosphorylated 25 kDa polypeptide of the light-harvesting complex of Photosystem II is encoded by the Type 2 cab-II genes. Biochim Biophys Acta BBA - Bioenerg 1019: 110–114

Järvi S, Suorsa M, Paakkarinen V, Aro E (2011) Optimized native gel systems for separation of thylakoid protein complexes: novel super- and mega-complexes. Biochem J 439: 207–214

Kim E, Ahn TK, Kumazaki S (2015) Changes in Antenna Sizes of Photosystems during State Transitions in Granal and Stroma-Exposed Thylakoid Membrane of Intact Chloroplasts in Arabidopsis Mesophyll Protoplasts. Plant Cell Physiol 56: 759–768

Kinoshita E, Kinoshita-Kikuta E, Koike T (2009) Separation and detection of large phosphoproteins using Phos-tag SDS-PAGE. Nat Protoc 4: 1513–1521

Kirchhoff H (2014) Structural changes of the thylakoid membrane network induced by high light stress in plant chloroplasts. Philos Trans R Soc Lond B Biol Sci 369: 20130225

Kouřil R, Dekker JP, Boekema EJ (2012) Supramolecular organization of photosystem II in green plants. Biochim Biophys Acta 1817: 2–12

Kouřil R, Zygadlo A, Arteni AA, de Wit CD, Dekker JP, Jensen PE, Scheller HV, Boekema EJ (2005a) Structural Characterization of a Complex of Photosystem I and Light-Harvesting Complex II of Arabidopsis thaliana†. Biochemistry (Mosc) 44: 10935–10940

Kouřil R, Zygadlo A, Arteni AA, de Wit CD, Dekker JP, Jensen PE, Scheller HV, Boekema EJ (2005b) Structural Characterization of a Complex of Photosystem I and Light-Harvesting Complex II of Arabidopsis thaliana†. Biochemistry (Mosc) 44: 10935–10940

Larsson UK, Sundby C, Andersson B (1987) Characterization of two different subpopulations of spinach light-harvesting chlorophyll ab-protein complex (LHC II): Polypeptide composition, phosphorylation pattern and association with Photosystem II. Biochim Biophys Acta BBA - Bioenerg 894: 59–68

Leoni C, Pietrzykowska M, Kiss AZ, Suorsa M, Ceci LR, Aro E-M, Jansson S (2013) Very rapid phosphorylation kinetics suggest a unique role for Lhcb2 during state transitions in Arabidopsis. Plant J 76: 236–246

Mekala NR, Suorsa M, Rantala M, Aro E-M, Tikkanen M (2015) Plants Actively Avoid State Transitions upon Changes in Light Intensity: Role of Light-Harvesting Complex II Protein Dephosphorylation in High Light. Plant Physiol 168: 721–734

Pagliano C, Nield J, Marsano F, Pape T, Barera S, Saracco G, Barber J (2014) Proteomic characterization and three-dimensional electron microscopy study of PSII–LHCII supercomplexes from higher plants. Biochim Biophys Acta BBA - Bioenerg 1837: 1454–1462

Pietrzykowska M, Suorsa M, Semchonok DA, Tikkanen M, Boekema EJ, Aro E-M, Jansson S (2014) The Light-Harvesting Chlorophyll a/b Binding Proteins Lhcb1 and Lhcb2 Play Complementary Roles during State Transitions in Arabidopsis. Plant Cell Online 26: 3646–3660

Pribil M, Pesaresi P, Hertle A, Barbato R, Leister D (2010) Role of Plastid Protein Phosphatase TAP38 in LHCII Dephosphorylation and Thylakoid Electron Flow. PLoS Biol 8: e1000288

Rochaix J-D (2014) Regulation and Dynamics of the Light-Harvesting System. Annu Rev Plant Biol 65: 287–309

Samol I, Shapiguzov A, Ingelsson B, Fucile G, Crèvecoeur M, Vener AV, Rochaix J-D, Goldschmidt-Clermont M (2012) Identification of a Photosystem II Phosphatase Involved in Light Acclimation in Arabidopsis. Plant Cell Online 24: 2596–2609

Schägger H, von Jagow G (1991) Blue native electrophoresis for isolation of membrane protein complexes in enzymatically active form. Anal Biochem 199: 223–231

Shapiguzov A, Ingelsson B, Samol I, Andres C, Kessler F, Rochaix J-D, Vener AV, Goldschmidt-Clermont M (2010) The PPH1 phosphatase is specifically involved in LHCII dephosphorylation and state transitions in Arabidopsis. Proc Natl Acad Sci U S A 107: 4782–4787

Standfuss J, Kühlbrandt W (2004) The Three Isoforms of the Light-harvesting Complex II SPECTROSCOPIC FEATURES, TRIMER FORMATION, AND FUNCTIONAL ROLES. J Biol Chem 279: 36884–36891

Wientjes E, van Amerongen H, Croce R (2013a) Quantum Yield of Charge Separation in Photosystem II: Functional Effect of Changes in the Antenna Size upon Light Acclimation. J Phys Chem B 117: 11200–11208

Wientjes E, Drop B, Kouřil R, Boekema EJ, Croce R (2013b) During State 1 to State 2 Transition in Arabidopsis thaliana, the Photosystem II Supercomplex Gets Phosphorylated but Does Not Disassemble. J Biol Chem 288: 32821–32826

Yokono M, Takabayashi A, Akimoto S, Tanaka A (2015) A megacomplex composed of both photosystem reaction centres in higher plants. Nat Commun. doi: 10.1038/ncomms7675

Zer H, Vink M, Shochat S, Herrmann RG, Andersson B, Ohad I (2003) Light Affects the Accessibility of the Thylakoid Light Harvesting Complex II (LHCII) Phosphorylation Site to the Membrane Protein Kinase(s)†. Biochemistry (Mosc) 42: 728–738

Zhang Y, Liu C, Liu S, Shen Y, Kuang T, Yang C (2008) Structural stability and properties of three isoforms of the major light-harvesting chlorophyll a/b complexes of photosystem II. Biochim Biophys Acta BBA - Bioenerg 1777: 479–487

Figure 1

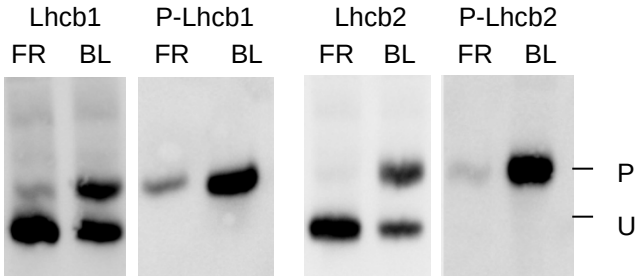

Two-layer Phos-tag PAGE resolves the phosphorylated and un-phosphorylated forms of Lhcb1 and Lhcb2.
Antisera against Lhcb1 or Lhcb2 recognize both bands, while phospho-specific antisera (P-Lhcb1 or P-Lhcb2) recognize only the slower migrating band, confirming that it represents the form that is phosphorylated at the N-proximal threonine. P and U indicate the phosphorylated and un-phosphorylated forms respectively.

Figure 2

A Lhcb1

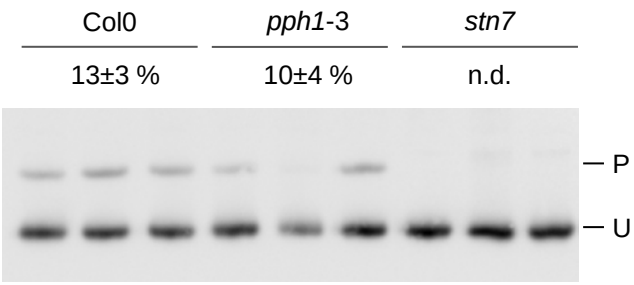

B Lhcb2

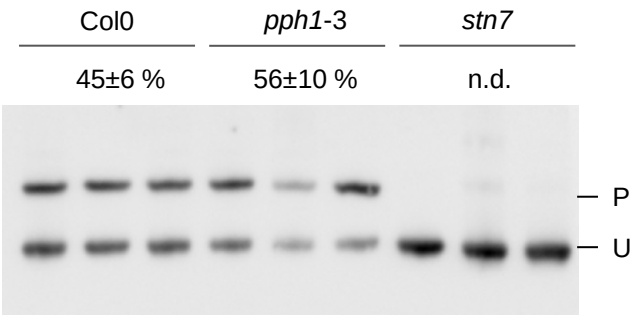

Lhcb phosphorylation in white light.
Total protein from mature leaves of 6-week old plants were subjected to two-layer Phos-tag™ PAGE. Three biological replicates are shown for each genotype. Wild type plants (Col0) are compared to the phosphatase mutant *pph1-3* and the kinase mutant *stn7*. The measured level of phosphorylation is indicated for each genotype above the immunoblots with the standard deviation (n=5). (n.d., <1% of phosphorylation). P and U indicate the phosphorylated and un-phosphorylated forms respectively.
A, Immunodetection of Lhcb1.
B, Immunodetection of Lhcb2.

Figure 3

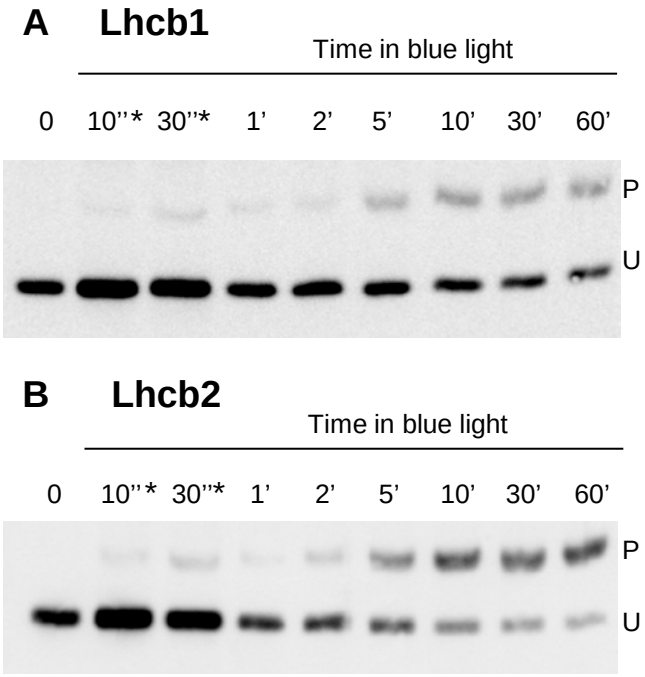

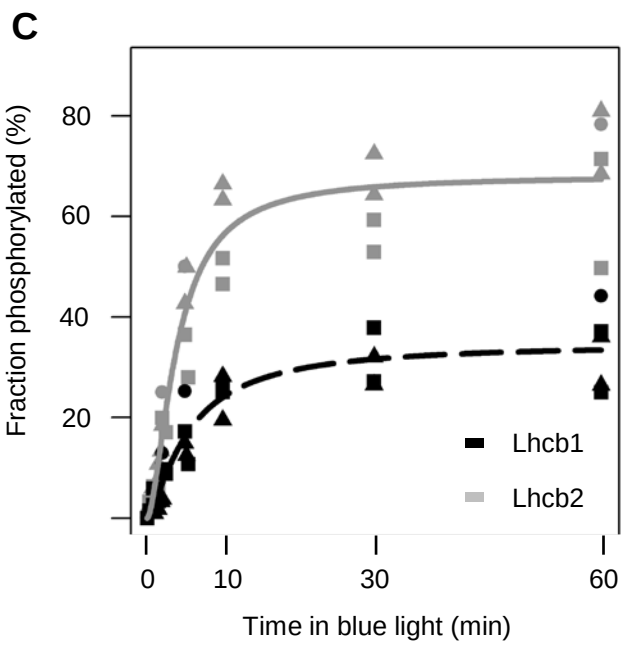

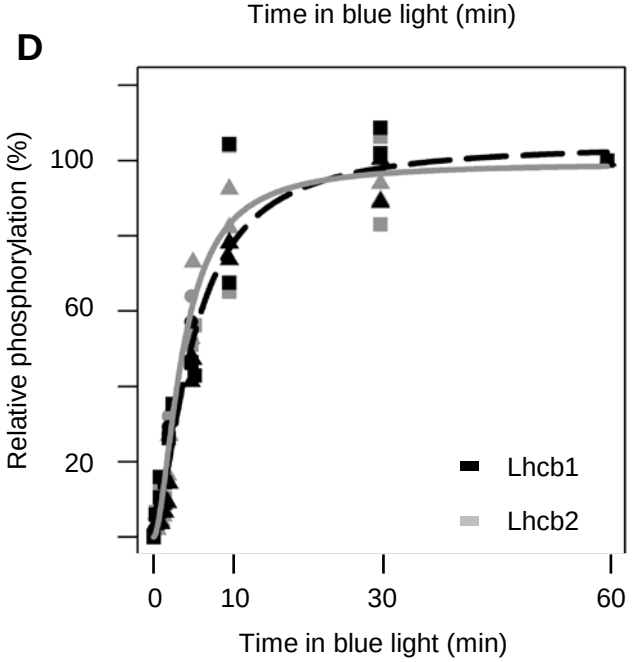

Phosphorylation kinetics upon a switch from far-red to blue light.
Total protein was extracted from 15-day old seedlings (three per time point) that were exposed to far-red light for 1 hour and then switched to blue light. The level of phosphorylation was determined at different times after the switch (time 0) to blue light.
A, Immunodetection of Lhcb1.
B, Immunodetection of Lhcb2.
C, Phosphorylation levels for Lhcb1 (dotted black line) and Lhcb2 (plain gray lines) of five samples such as those presented in panels A and B are plotted as a function of time. The lines represent a sigmoidal fit of the data. Triangles, squares and circles represent distinct biological replicates of the experiment.
D, The same data as in C are normalized to the final phosphorylation level (phosphorylation at t= 3600 s equals 100 %).

Figure 4

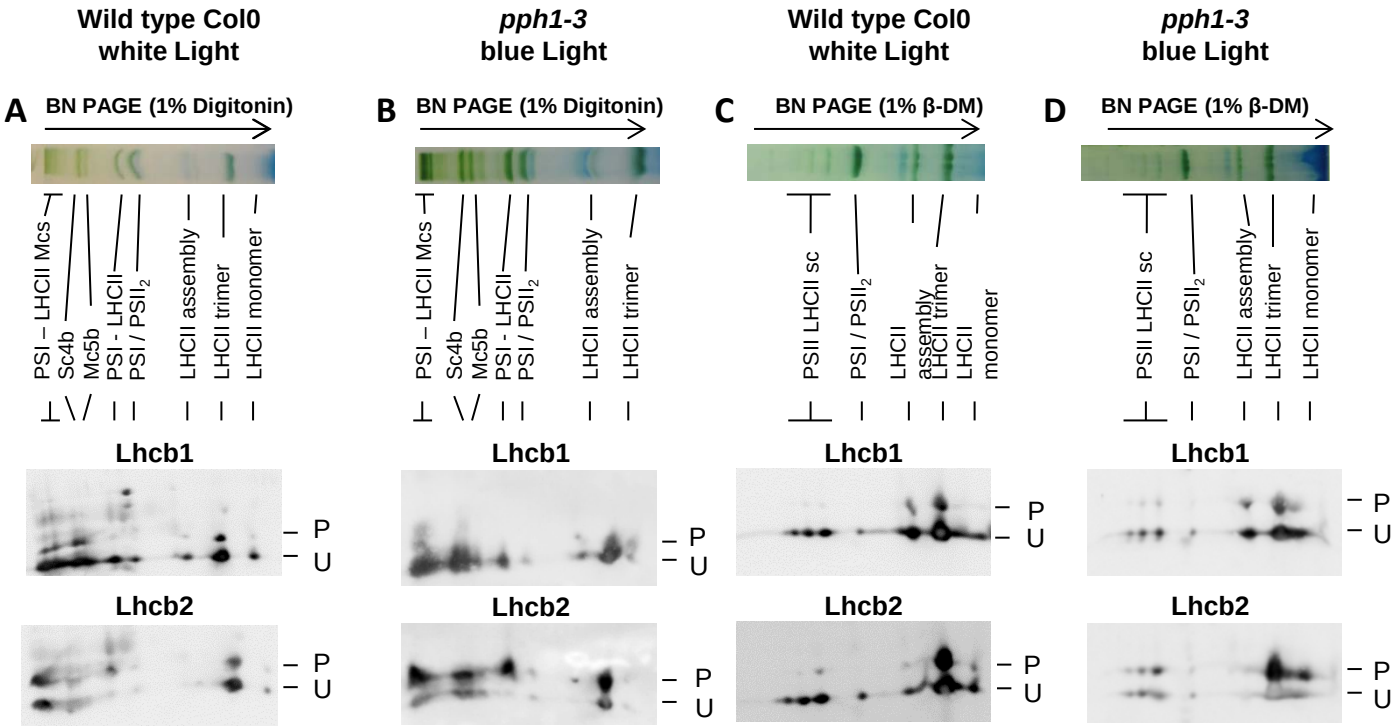

Lhcb1 and Lhcb2 phosphorylation in different supercomplexes.
Wild-type Col0 plants were grown under white light (70 µmol sec^{-1} m^{-2}) and harvested 4 hours after the onset of light. Thylakoid membranes were solubilized and subjected to Blue Native PAGE in the first dimension (shown at the top). The lanes were then subjected to a second dimension of two-layer Phos-tag™ PAGE and immunoblotting to reveal the phosphorylation of Lhcb1 and Lhcb2 (P, phosphorylated; U, un-phosphorylated).
A, Col-0 wild-type plants were grown in white light. Thylakoid membranes were solubilized with digitonin.
B, Mutant *pph1-3* plants were treated with far red light (1 hour) and then blue light (30 minutes) to increase antenna phosphorylation. Thylakoid membranes were solubilized with digitonin.
C, Col-0 plants were grown in white light as in A and thylakoid membrane were solubilized with β-DM.
D, Mutant *pph1-3* were treated as in panel B, and thylakoid membranes were solubilized with β-DM.
The bands are labelled as described by Järvi et al. (2011): Mcs, megacomplexes; Sc4b, supercomplex 4b; Mc5b, megacomplex 5b; PSI-LHCII, STN7-dependent PSI-LHCI-LHCII supercomplex; $PSI/PSII_2$, comigrating PSI-LHCI and PSII dimer; LHCII assembly, LHCII complex containing an LHCII trimer associated with monomeric Lhcbs (mainly Lhcb4 and Lhcb6); PSII LHCII sc, PSII dimer-LHCII supercomplexes.

Figure 5

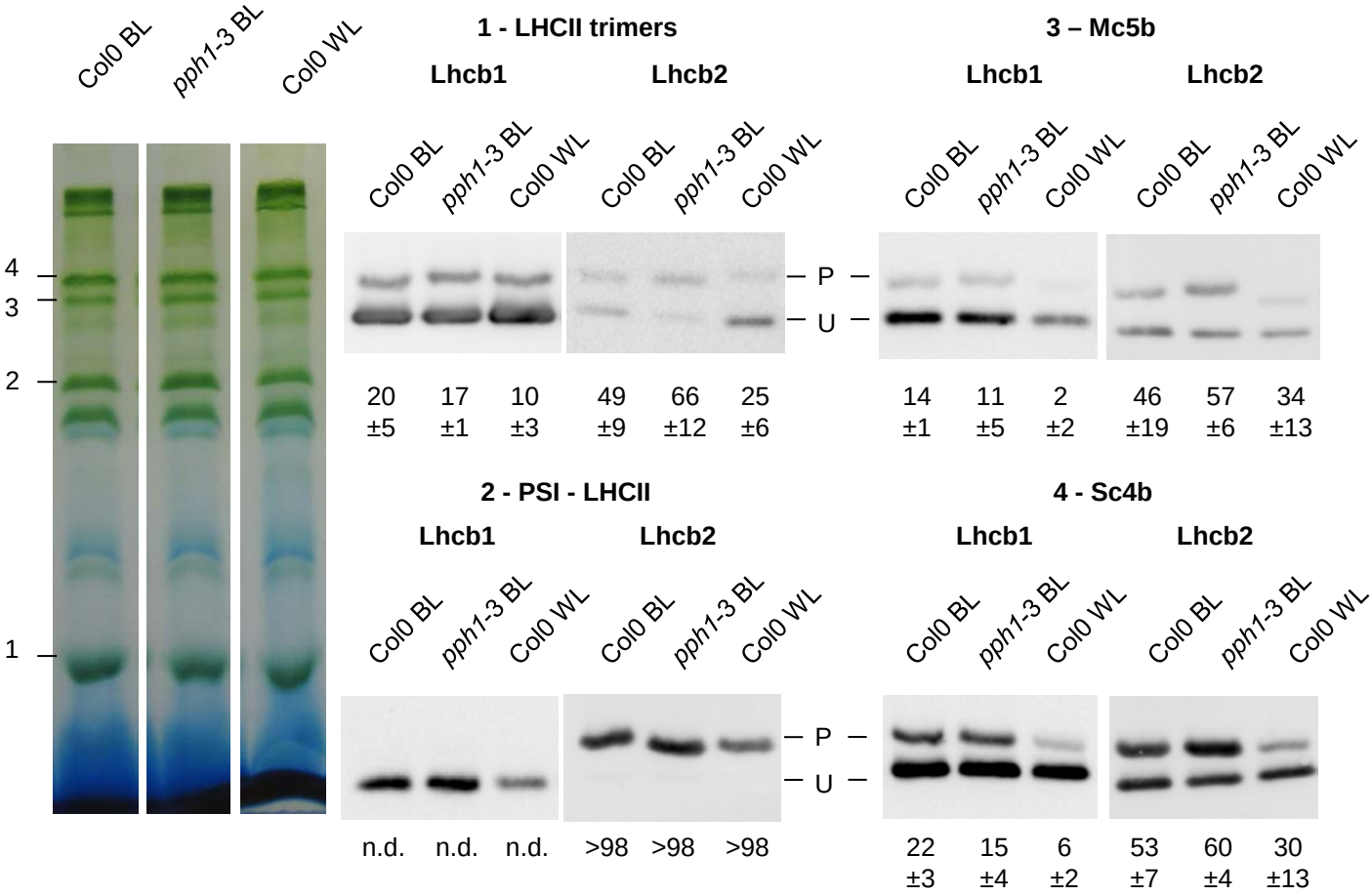

Quantification of Lhcb1 and Lhcb2 phosphorylation in supercomplexes.
Wild-type Col0 and mutant *pph1-3* plants were treated for 1 hour with far-red light and then exposed to blue light for 30 minutes (BL). Wild-type Col0 were also grown under white light (70 µmol sec^{-1} m^{-2}) and harvested 4 hours after the onset of light (WL). Thylakoid membrane complexes extracted with digitonin were subjected to BN PAGE. Individual bands were cut as indicated on the left (1-4) and separately analyzed by two-layer Phos-Tag™ PAGE and immunoblotting. The measured percentage of phosphorylation is indicated below each lane with its standard deviation (n=3). (n.d. < 1% phosphorylation)

Figure 6

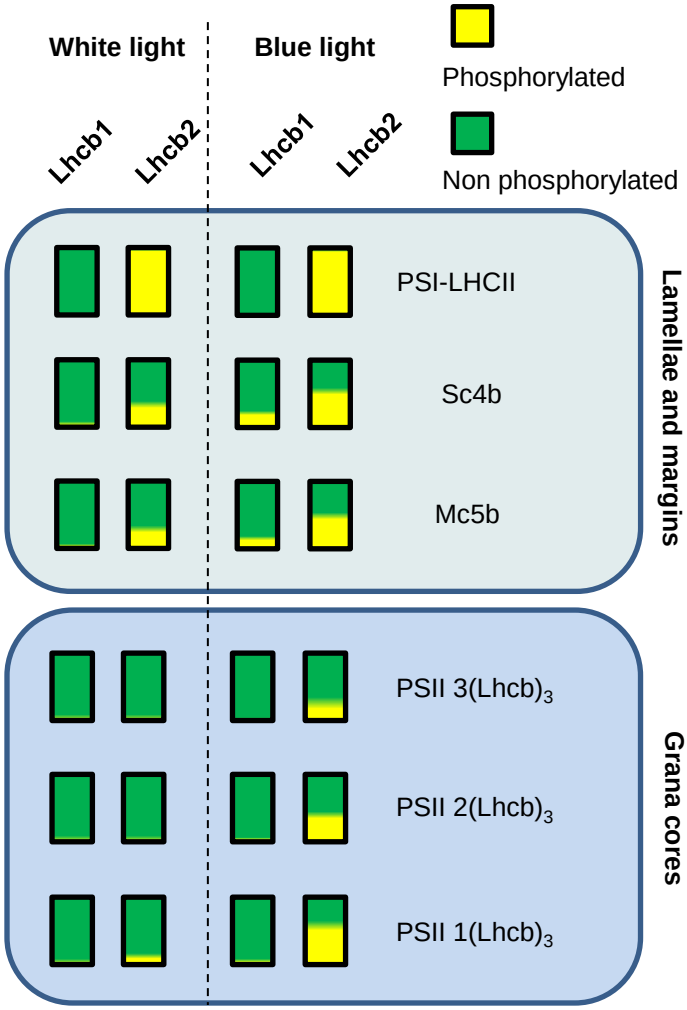

Lhcb1 and Lhcb2 phosphorylation in different supercomplexes.
The extent of phosphorylation of Lhcb1 and Lhcb2 is depicted for the supercomplexes present in the stromal lamellae and grana margins (upper box, digitonin extraction) and those present in the grana cores (lower box, β-DM extraction). In each bar, yellow represents the proportion of phosphorylated Lhcb1 or Lhcb2 and green the un-phosphorylated fraction. Plants grown under white light (left of the dotted line) are compared to plants shifted to blue light after a far-red treatment to increase overall antenna phosphorylation (right of the dotted line). The complexes are labelled on the right (Järvi et al. 2011): PSI-LHCII, STN7-dependent PSI-LHCI-LHCII supercomplex, Sc4b, supercomplex 4b; Mc5b, megacomplex 5b ; PSII-3(Lhcb)$_3$, PSII-LHCII supercomplex containing 3 LHCII trimers; PSII-3(Lhcb)$_2$, PSII-LHCII supercomplex containing 2 LHCII trimers; PSII-1(Lhcb)$_3$, PSII-LHCII supercomplex containing 1 LHCII trimer.

Supplemental figure 1

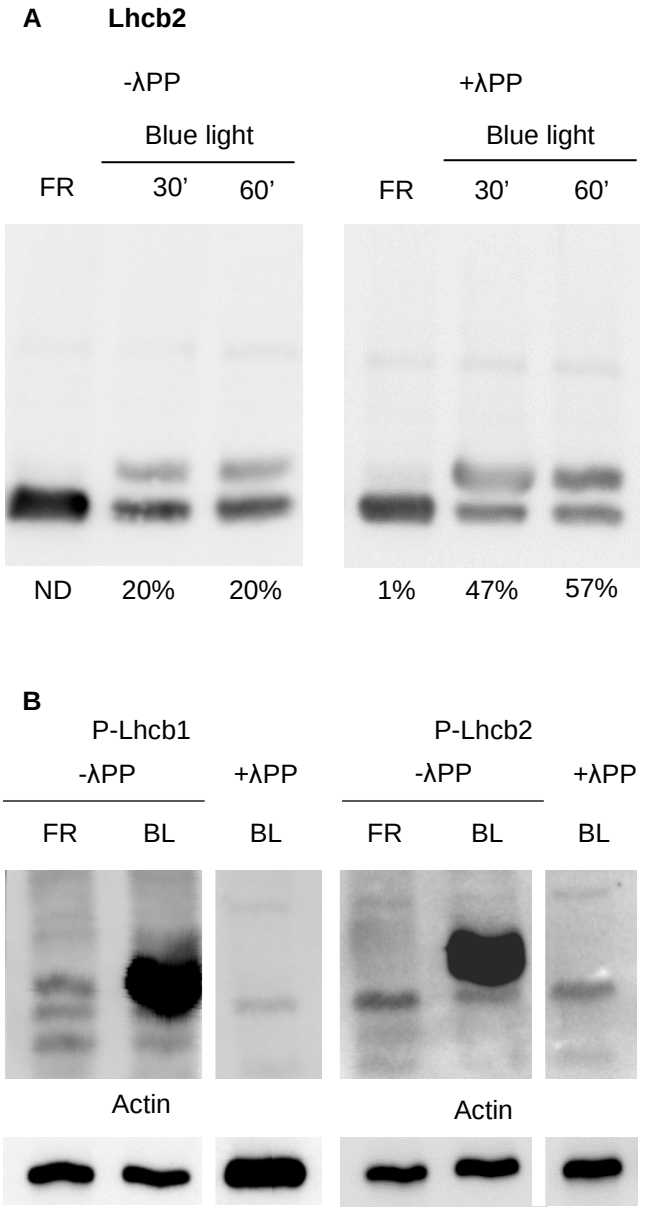

Phosphatase treatment enhances detection of the phosphorylated form of Lhcb2.
A, Prior to immunodetection with antiserum against Lhcb2, replicate membrane blots were incubated in phosphatase buffer in the presence (+λPP) or absence (-λPP) of λ protein phosphatase. The signal for the phosphorylated form of Lhcb2 increases more than two-fold after treatment with the phosphatase, indicating that phosphorylation severely hampers the recognition of P-Lhcb2 by the Lhcb2 antiserum. Total proteins were extracted from 6 weeks old plants exposed to far-red light for 1 hour (FR) and then shifted to blue light (BL) for 30 or 60 minutes. The average fold-increase of the apparent phosphorylation level after the phosphatase treatment was 2.25 ± 0.31 (n=3).
B, To test whether dephosphorylation of proteins on the membrane blot by λ phosphatase was complete, replicate membrane blots were incubated with λ protein phosphatase (+λPP) or untreated. They were then immune-decorated with phospho-specific antibodies against P-Lhcb1 or P-Lhcb2 as indicated at the top. A long exposure is presented to highlight the absence of detectable signal on the phosphatase-treated membranes while the signal is saturating on the untreated membranes. The FR and BL (60') samples are the same as in panel A.

Supplemental figure 2

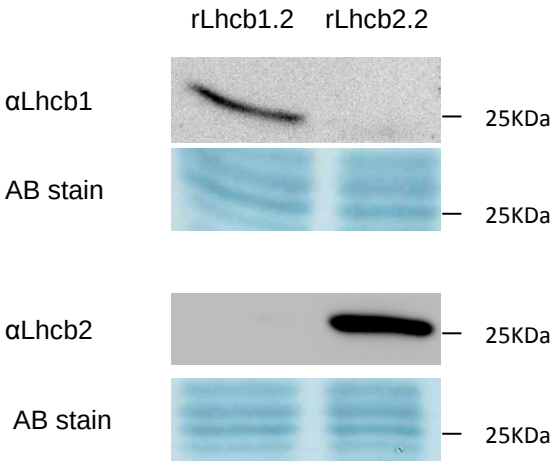

Specificity of the Lhcb1 and Lhcb2 antibodies against recombinant proteins.
Antibodies against Lhcb1 or Lhcb2 were tested by immunoblotting of crude E.coli extracts expressing the recombinant proteins Lhcb1.2 or Lhcb2.3. The staining with amido black (AB stain) is shown to confirm the loading.

Methods.
The coding sequences were obtained from the TAIR repository (Lhcb1.2 - U17058 Lhcb2.3 – U16031) and assembled into the pET28a vector (Novagen) between the *Nco*I and *Xho*I sites with the following primers:
Lhcb1.2 FOR: GTTTAACTTTAAGAAGGAGATATACCATGGATGAGGAAGACTGTTGCCAAGC
Lhcb1.2 REV: CTCAGTGGTGGTGGTGGTGGTGCTCGAGCTTTCCGGGAACAAAGTTGGTTGC
Lhcb2.3 FOR: GTTTAACTTTAAGAAGGAGATATACCATGCGTCGTACCGTCAAGT
Lhcb2.3 REV: CTCAGTGGTGGTGGTGGTGGTGCTCGAGTTTTCCGGGGACGAAGTTGGTG.

Cultures were grown in LB media (Sigma-Aldrich) to the optical density of 0.5-0.6 at 600 nm. Protein expression was then induced with 0.5mM IPTG for 4h at 28°C. The pellets were resuspended in lysis buffer (100mM Tris-HCl pH 7.8 2% SDS, 1x protease inhibitors (P8849 - Sigma-Aldrich)), sonicated 10 times for 10 seconds and centrifuged for 5 minutes at 18000 g. The supernatant was collected and diluted with 4x loading buffer (10% SDS, 40% Sucrose, 1mM EDTA, 20% 2-Mercaptoethanol, 62.5mM Tris-HCl pH 6.8). The amount of protein was corrected on the basis of coomassie staining of the samples after SDS-PAGE. After the separation on 10% acrylamide/bis-acrylamide gel the protein were transfered to a nitrocellulose membrane and treated as described in Methods for the Two-layer Phos-tag™ PAGE except that the λ protein phosphatase treatment was not performed.

Supplemental figure 3

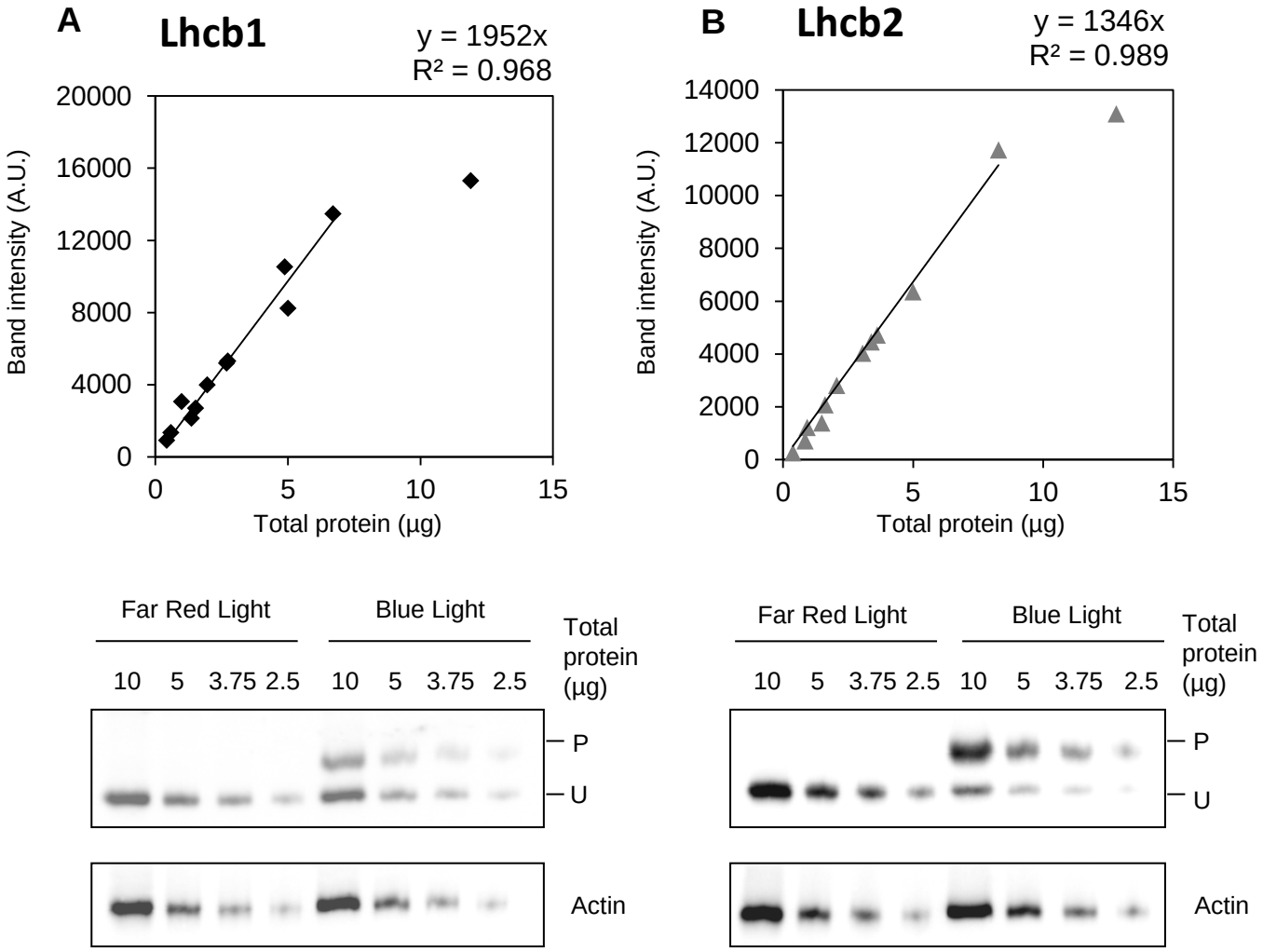

Determination of the linear range of the immunoblot assay.
Different amounts of total protein (as indicated at the top of the immunoblots and plotted on the x axis) were subjected to two-layer Phos-tag™ PAGE. The signal measured by immunoblotting (integration of pixel intensities for each band), normalized to the signal obtained with actin antiserum, is plotted on the y axis. The samples are total protein extracts from plants subjected to far red or blue light, as indicated. All the signals from phosphorylated (P) and unphosphorylated (U) forms are plotted after normalizing to the signal of actin.

Supplemental figure 4

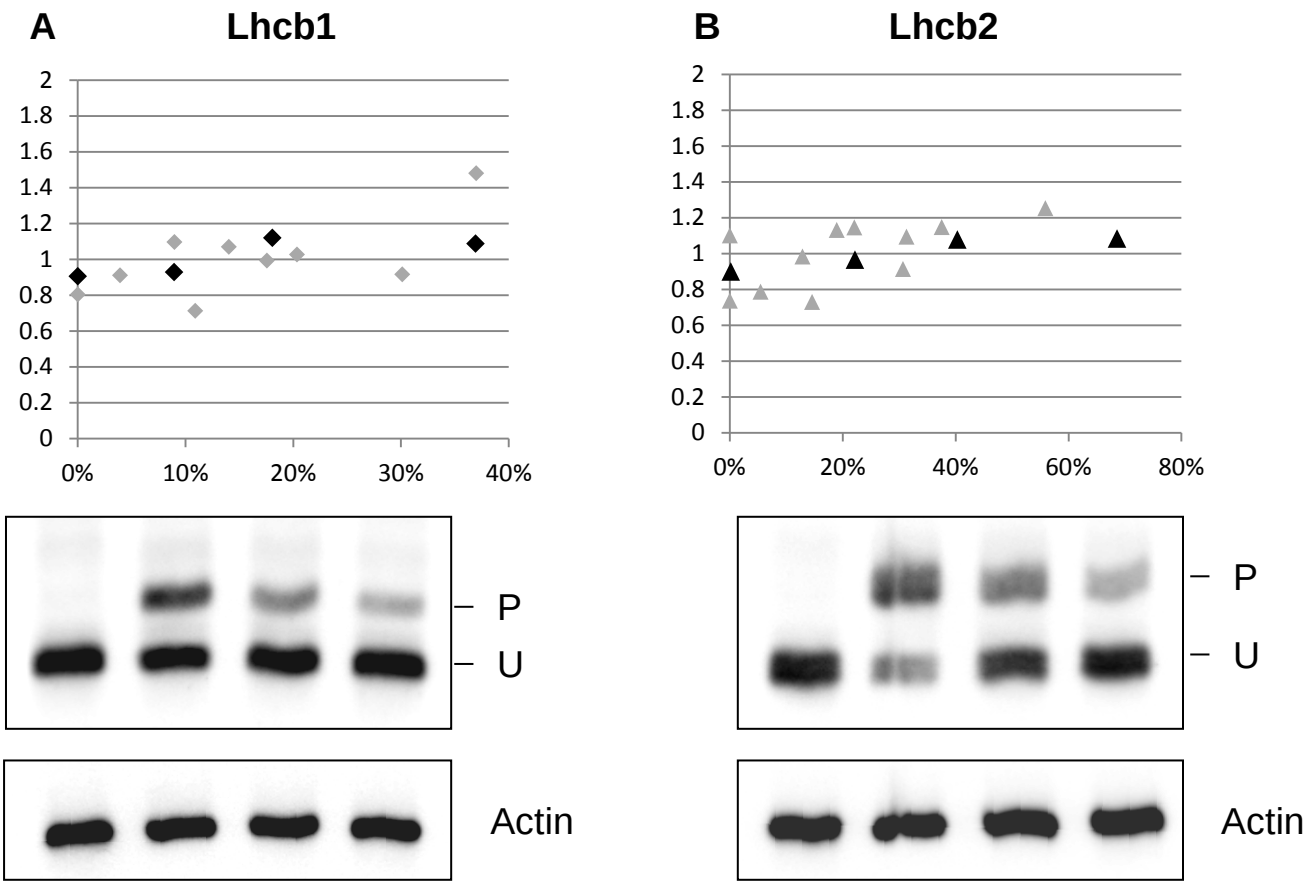

Phosphorylated and non-phosphorylated Lhcb1 or Lhcb2 are detected with similar efficiency.
The sum of the band intensities for the phosphorylated (P) and non-phosphorylated (U) forms of Lhcb1 (A) or Lhcb2 (B) were normalized to the intensity of the actin band. The normalized sum (y axis) does not change with different extents of phosphorylation (x axis), confirming that there is no specific retention of the phosphorylated proteins during transfer from the gel to the immunoblot membrane. Samples with different extents of Lhcb phosphorylation were obtained by mixing different amounts of protein extract from plants exposed for 30 minutes to blue light with protein extracts from plants treated with far-red light for 1 hour (black symbols) or by taking samples at different time points of exposure to blue light (gray symbols).

Supplemental figure 5

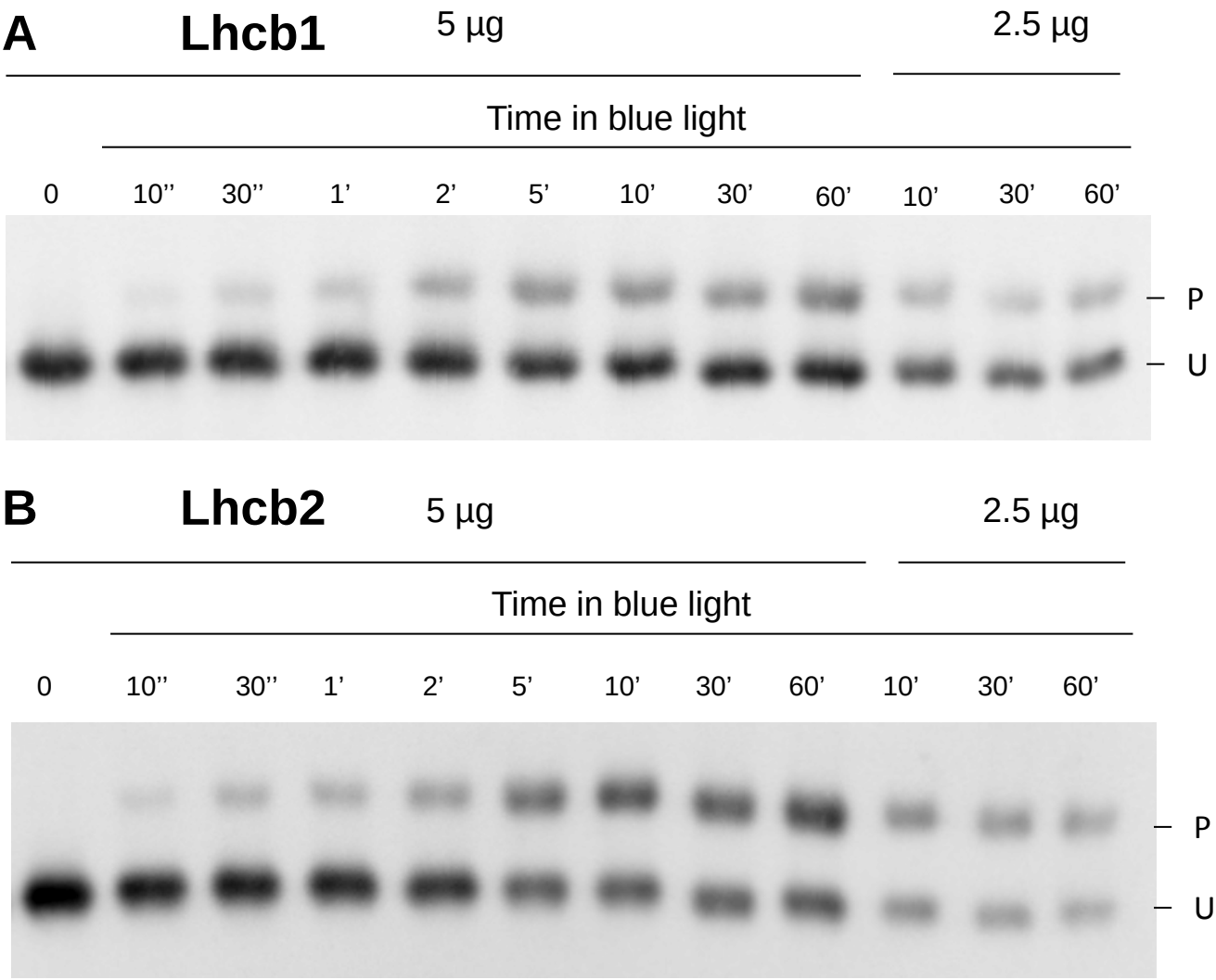

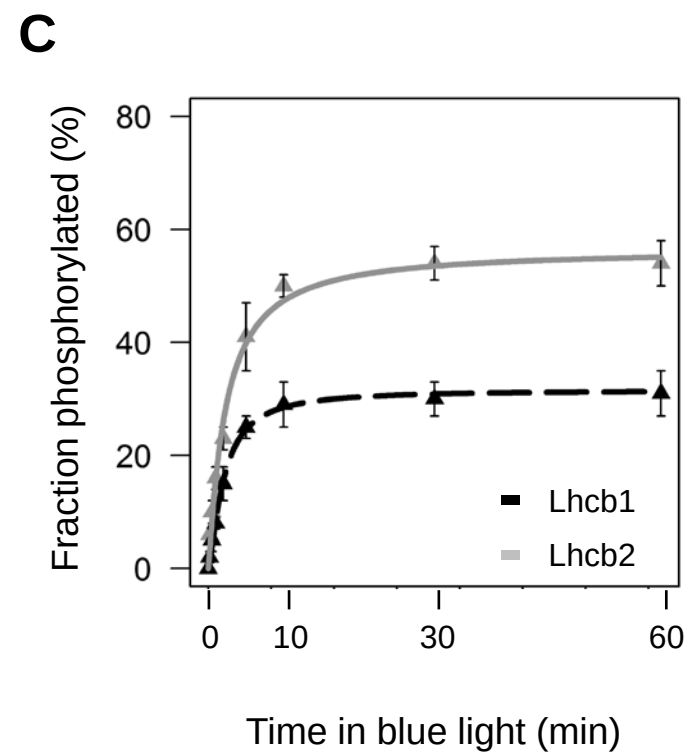

Phosphorylation kinetics in leaves of 6-week old Arabidopsis plants.
A and B, Phosphorylation kinetics of Lhcb1 and Lhcb2 were determined by two-layer Phos-tag™ PAGE upon a shift (at time 0) from far red light (state 1) to blue light (state 2) for Lhcb1 (A) and Lhcb2 (B).
C, The extent of phosphorylation of Lhcb1 (black points) and Lhcb2 (gray points) in panels A and B respectively is plotted as a function of time. Total proteins were extracted from mature leaves of two different plants for each time point. Error bars represent the standard deviation of three replicate experiments. The lines represent the sigmoidal interpolation of the points for Lhcb1 (dashed black line) and Lhcb2 (plain gray line).

Supplemental figure 6

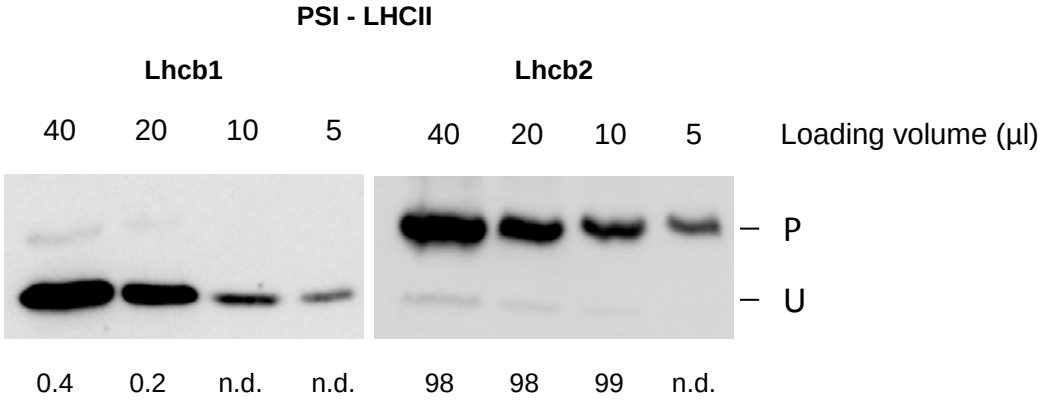

Evaluation of phosphorylation levels of Lhcb1 and Lhcb2 in the PSI-LHCII supercomplex.
Bands corresponding to the PSI-LHCII supercomplex were extracted as in Figure 5. A series of decreasing volumes were loaded as shown at the top. The presence of the less abundant bands can be detected only at larger loadings (phosphorylated Lhcb1 and unphosphorylated Lhcb2). Due to the saturation of the stronger signal the quantification for these fractions can not be accurately performed, the apparent percentage of phosphorylation is reported below. (n.d., not detectable). Thus a conservative estimate is that in the PSI-LHCII complex, Lhcb1 phosphorylation is <1% and Lhcb2 phosphorylation is >98%.

Supplemental figure 7

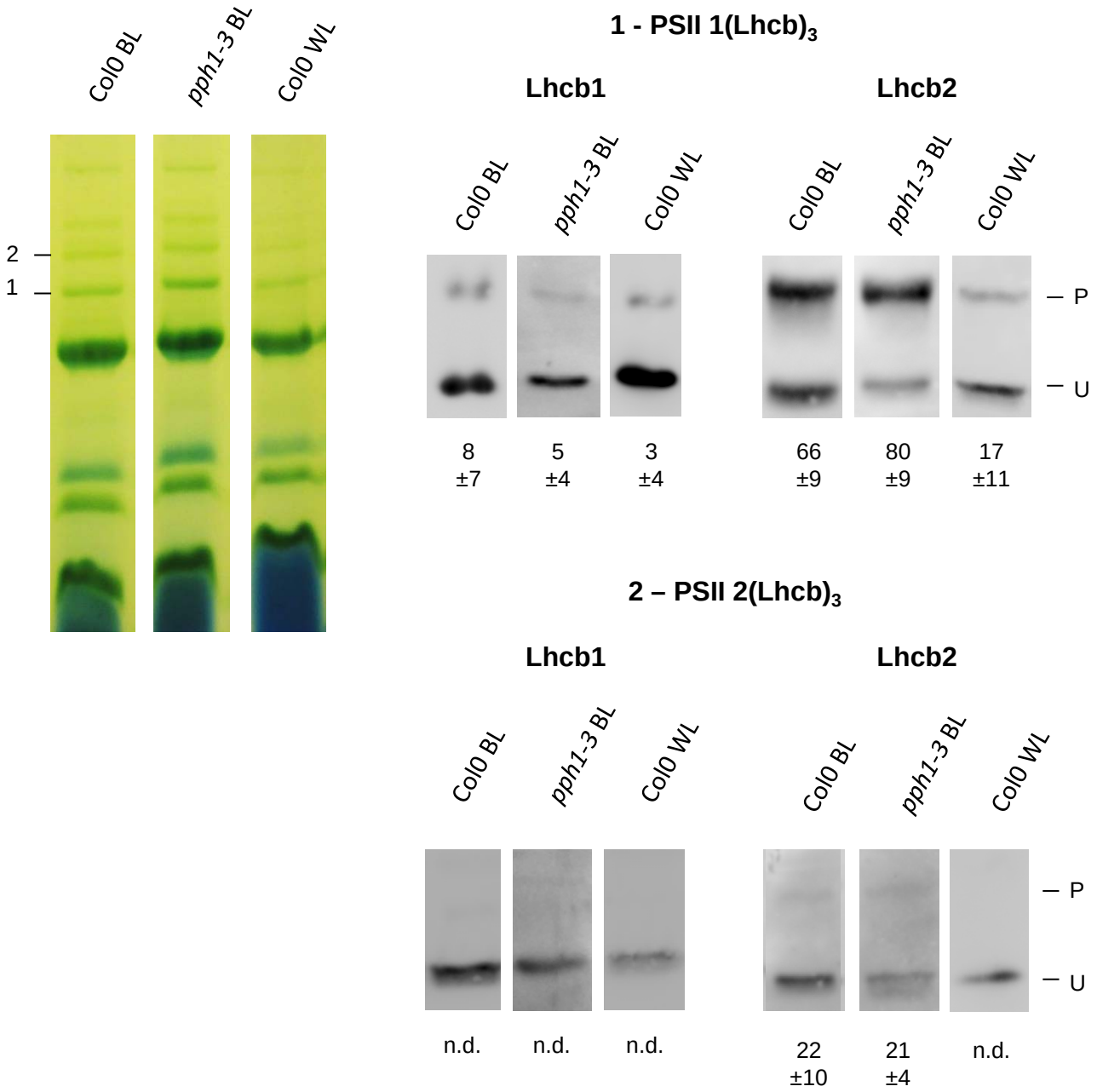

Quantification of Lhcb1 and Lhcb2 phosphorylation in PSII-LHCII supercomplexes.
Wild-type Col0 and mutant *pph1-3* plants were treated for 1 hour with far-red light and then exposed to blue light for 30 minutes (BL). Wild-type Col0 were also grown under white light (70 µmol sec^{-1} m^{-2}) and harvested 4 hours after the onset of light (WL). Thylakoid membrane complexes extracted with β-dodecylmaltoside were subjected to BN PAGE. Individual bands were cut as indicated on the left (1-2) and separately analyzed by two-layer Phos-Tag™ PAGE and immunoblotting. In band 1 (PSII 1$(Lhcb)_3$) the PSII dimer is associated with 1 LHCII trimer, in band 2 (PSII 2$(Lhcb)_3$) with 2 trimers.
The measured percentage of phosphorylation is indicated below each lane with its standard deviation (n=4). (n.d. non determined, i.e. < 1% phosphorylation)